Massi et al. survey of low-luminosity sources in the Vela D cloud has a slightly lower sensitivity. The maximum stellar masses in the Vela clusters have been computed assuming that a fraction of the total luminosity ranging from 30% to 100% is emitted by the most massive object. The young IRAS sources in the Vela molecular cloud show the same trend as the Herbig Ae/Be stars: more massive stars are surrounded by rich clusters, while low-mass stars are found in relative isolation.

In the same plot, the result of the various surveys are compared with the predictions of a "random sampling model" (as described in Testi et al. 2001). Our results clearly deviate from the prediction of the model, since no massive object is found in isolation, and all lie above the median predictions of the model. These results suggest that there is a physical connection between clusters and high-mass stars. This does not necessarily *imply* that massive stars are formed by coalescence in (proto-)cluster environments, but suggests that the conditions to form a massive star are such that this process is associated with the formation of a cluster of (lower-mass) objects. The cluster could be either the catalyst of high-mass star formation or a by-product of it.

These conclusions should and will be made more firm by combining larger samples from various surveys toward different regions.

References

Bonnell I. A., & Clarke C. J., 1999, *MNRAS*, **309**, 461.

Clarke C. J., Bonnell I. A., & Hillenbrand L. A., 2000, in Protostars and Planets IV, eds. V. Mannings, A. Boss & S. S. Russell (Tucson: University of Arizona press), p. 151.

Gomez M., Hartmann L., Kenyon S. J., Hewett R., 1993, *AJ*, **105**, 1927.

Hillenbrand L. A. & Hartmann L. W., 1998, *ApJ*, **492**, 540.

Hillenbrand L. A. & Carpenter J. M., 2000, *ApJ*, 540, 236.

Liseau R., Lorenzetti D., Nisini B., Spinoglio L., Moneti A., 1992, *A&A* **265**, 577.

Massi F., Lorenzetti D., Vitali F.: "Near Infrared H2 imaging of YSOs in Vela Molecular Clouds" in Malbet F., Castets A. (eds.), Low Mass Star Formation from Infall to Outflow – Poster Proceedings of the IAU Symposium n. 182 on Herbig-Haro Flows and the Birth of Low Mass Stars, Observatoire de Grenoble 1997.

Massi F., Giannini T., Lorenzetti D. et al., 1999, *A&AS* **136**, 471.

Massi F., Lorenzetti D., Giannini T., Vitali F., 2000, *A&A* **353**, 598.

Murphy D. C., May J., 1991, *A&A* **247**, 202.

Palla F. & Stahler S.W., 1999, *ApJ*, **525**, 772.

Testi L., Palla F., Natta A., 1998, *A&AS*, **133**, 81.

Testi L., Palla F., Natta A., 1999, *A&A*, **342**, 515.

Testi L, Palla F., Natta A., 2001, in "From Darkness to Light", eds. T. Montmerle and Ph. André, ASP Conf. Series, in press.

Building Luminous Blue Compact Galaxies by Merging

P. AMRAM[1] AND G. ÖSTLIN[2]

[1]Observatoire de Marseille, France; [2]Stockholm Observatory, Sweden

ABSTRACT

Observations of six luminous blue compact galaxies (LBCGs) and two star-forming companion galaxies were carried out with the CIGALE scanning Fabry-Perot interferometer attached to the ESO 3.6-m telescope, targeting the Hα emission line. The gaseous velocity field presents large-scale peculiarities, strong deviations to pure circular motions and sometimes, secondary dynamical components. In about half the cases, the observed rotational velocities are too small to allow for pure rotational support. If the gas and stars are dynamically coupled, a possible explanation is either that velocity dispersion dominates the gravitational support or the galaxies are not in dynamical equilibrium, because they are involved in mergers, explaining the peculiar kinematics. In two cases, we find evidence for the presence of dark matter within the extent of the Hα rotation curves and in two other cases we find marginal evidence. For most of the galaxies of the present sample, the observed peculiarities have probably as origin merging processes; in five cases, the merger hypothesis is the best way to explain the ignition of the starbursts. This is the most extensive study as yet of optical velocity fields of luminous blue compact galaxies.

1. Introduction

A Blue Compact Galaxy (BCG) is characterised by blue optical colours, $-21 < M_B < -12$, an HII-region-like emission-line spectrum, a compact appearance on photographic sky-survey plates, small to intermediate sizes, high star-formation rates per unit luminosity and low chemical abundances (e.g. Searle and Sergent, 1972). Moreover, most BCGs are rich in neutral hydrogen. There is no consensus on the process(es) that trigger the bursts of star formation. Three main scenarios have been proposed to explain it: (1) cyclic infall of cooled gas: Starbursts are terminated by SN winds, but when gas later accretes back, a new starburst may be ignited; (2) galaxy interactions and (3) collapse of protocloud if BCGs are genuinely young galaxies. Most arguments have been based on photometry alone. On the other hand, the dynamics of these systems are not well explored, still the creation of an energetic event like a sudden burst of star formation is likely to have dynamical causes and impacts, complicating the interpretation.

To improve our understanding of the dynamics and the triggering mechanisms behind the starburst activity, we have obtained Fabry-Perot data allowing us to achieve two-dimensional velocity fields with both high spatial and spectral (velocity) resolutions. BCGs are obviously the galaxies for which 2-D data are absolutely requested due to the non-axisymmetry of the velocity field around the centre of mass.

The selected BCGs are among the more luminous ones known in the nearby universe. The galaxies were observed at the Hα-emission line with the ESO 3.6-m telescope on La Silla. The exposure times ranged between 24 minutes and 160 minutes. In Östlin et al. (1999), we presented and described the data: Hα images, velocity fields, continuum maps and rotation curves. In

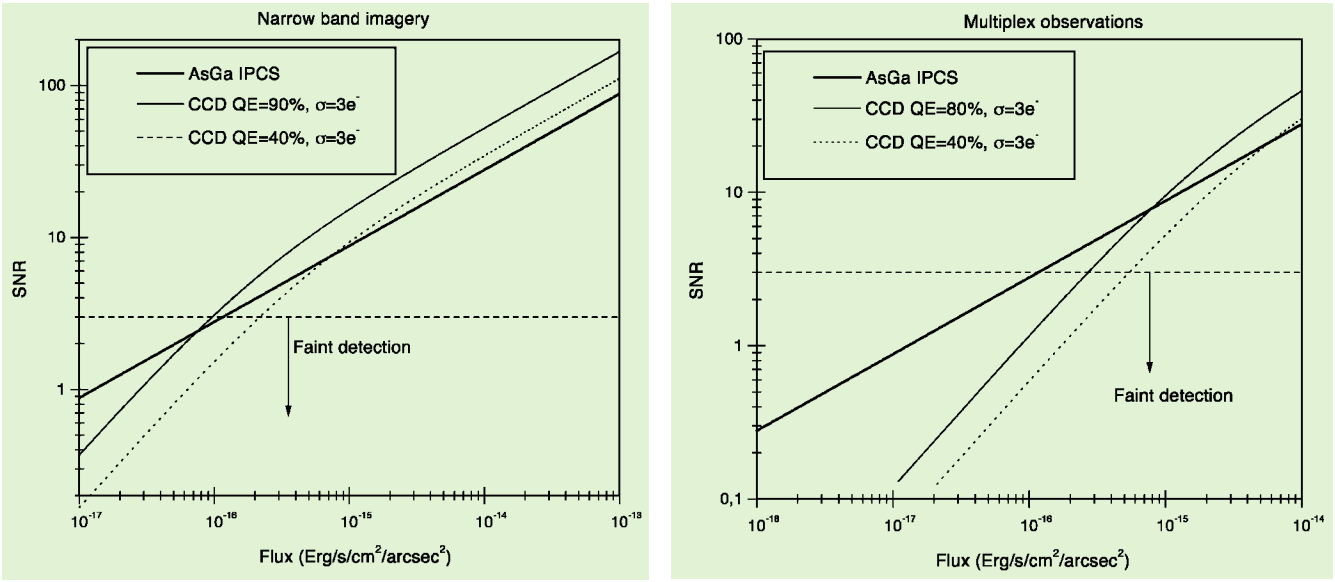

Figure 1: Comparison of the performances, expressed in terms of signal-to-noise ratio vs. the flux of the extended source for two CCDs (with different quantum efficiency) and an AsGa IPCS in a narrow-band imaging application (left) and in a multiplex application like a scanning Fabry-Perot interferometer (right). See text for further details.

Östlin et al. (2001), we will discuss the interpretation of these observations and their implications on the dynamics, the mass distribution and the triggering mechanism behind the starbursts.

In this paper, we give a flavour of the observations and provide some descriptions of two galaxies: ESO 350-IG38 and ESO 338-IG04. Then, we point out the hot spots of the sample and suggest an interpretation.

2. A Scanning Fabry-Perot Interferometer on the ESO 3.6-m

The instrument CIGALE attached to the Cassegrain focus of the ESO 3.6-m was used for the observations. CIGALE is basically composed of a focal reducer, a scanning Fabry-Perot interferometer, an interference filter and an IPCS (Image Photon Compting System). CIGALE (for Cinématique des GALaxiEs) is a visiting instrument belonging to Marseille Observatory, mounted for the first time on the ESO 3.6-m in 1991 and commissioned on the average for one run a year since that time. (In fact, a Fabry-Perot etalon plus an image tube has been mounted on the ESO 3.6-m by the Marseille team for the first time in 1979, see Marcelin et al., 1982). With the efficient cooperation of the 3.6-m ESO team and of the astro-workshop, using the facilities of the telescope, the instrument is easily mounted during the daytime of the first observing night. Several replica of this instrument exist throughout the world, one of them is presently extensively used on the OHP 1.93-m telescope (Observatoire de Haute-Provence, France) to provide a sample of about 200 velocity fields of nearby galaxies (the GHASP's project – Gassendi HAlpha SPiral galaxies survey – see http://www-obs.cursmrs.fr/interferometrie/GHASP/ghasp.html). The instrument CIGALE based at La Silla is used both on the ESO 3.6-m and on the Marseille 36-cm telescope. On the Marseille telescope, CIGALE has a wide field of view (40 arcmin square) and is used to make a kinematical deep Hα survey of gaseous emission regions in the Milky Way and in the Magellanic Clouds (see for instance Georgelin et al., 2000). On the 3.6-m, CIGALE has a one hundred times smaller field (~ 4 arcmin square, providing a pixel size of 0.91 arcsec). The spectral scanning step depends on the interferometer used, it was of 4.8 km s^{-1} for the present study. A full description of the instrument CIGALE is given in a previous paper in *The Messenger* (Amram et al., 1991). By the way, a previous discussion in *The Messenger* on BCGs (Infants of the Universe?) including ESO 338-IG04 can be found in Bergvall & Olofsson (1984). Data reduction was performed using the http available ADHOCw software (http://www-obs.cnrs-mrs.friadhoc/adhoc.html); a complete data-reduction procedure is given for instance in Amram et al. (1991, 1996). In August 1999 and in September 2000, two major upgrades were realised on CIGALE: the data-acquisition system and the receptor were removed. (1) Two hundred kg of electronics were substituted by a Matrox board allowing the acquisition of frames 1024 × 1024 px^2 at high frequency and the computation in real time of the events on each frame. (2) The 20-year old Thomson IPCS was replaced by a new AsGa IPCS. The semi-conductor photocathode AsGa (built by Hamamatsu) of the new detector offers a d.q.e. five times higher (25% instead of 5% for the old Thompson IPCS). The output of the AsGa tube is coupled by optical fibers to a 1024 × 1024 CCD. (http://www.obs.cnrs-mrs.fr/interferometrie/instrumentation.html#AsGa). The IPCS, with a time resolution of 1/50 second and zero readout noise makes it possible to scan the interferometer rapidly, avoiding problems with varying sky transparency, airmass and seeing during long exposures; and thus has several advantages over a CCD for this application. Figure 1 compares the total efficiency of a CCD and an IPCS used in narrow-band imaging (left) and in multiplex application (right). It clearly shows that at low intensity level, the signal-to-noise ratio is much higher with an IPCS than with a CCD in the case of multiplex observations as for instance scanning Fabry-Perot interferometry. Figure 1 has been plotted from a simulation of one hour exposure time on an 8-metre telescope, for a pixel size of 0.25 arcsec square, 48 scanning channels, transmissions of: 80% for the atmosphere; 64% for the 2 mirrors of the telescope; 70% for the interference filter; 80% for the optics and 90% for the Fabry-Perot (Gach et al., 2001). The data presented here were obtained in August 1995 with the old system; new observations were performed for another 15 BCGs, extending down to fainter luminosities in 1999 and 2000 with the new system, this will allow us to obtain a more comprehensive picture on the evolution of BCGs.

3. Results: Description of Two BGCs

3.1 ESO 350-IG38 (Haro 11)

The morphology of this object is complex. The three bright starburst nuclei are composed of numerous individual super star clusters ($M_V \geq -15$, Östlin, 2000) as it can be seen for an HST/WFPC2 image (Fig. 2 – left,

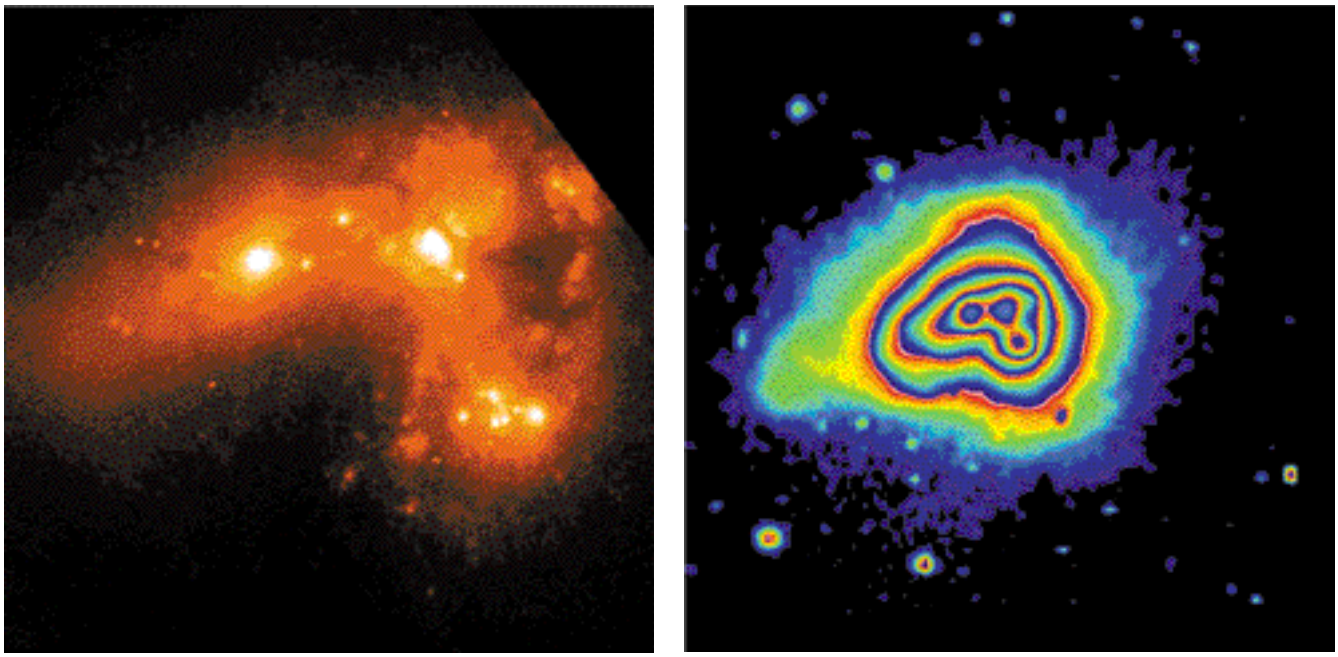

Figure 2: ***ESO 350-IG38.*** *North is up, East is left. (Left): HST/WFPC2 V+R (F606W) broad-band image. The scale of the box is 24 arcsec square. (Right): R-band CCD image. Note the irregular morphology at all isophotal levels. The faintest visible structures are* $\mu_R \approx 26$ *mag/arcsec*^{2}*. The size of the field is 1 by 1 arcminute, corresponding to 23 × 23 kpc.*

Malkan et al. 1998). The properties of the central regions bear a close resemblance with the classical colliding galaxies NGC 4038/4039 as seen in HST data (Whitmore and Schweizer 1995). This galaxy is the most massive in the whole sample and also has the highest star-formation rate (~ 20 $M_\odot$/yr). The inferred supernova (SN type II) frequency is one every 7 years. Surprisingly, the galaxy is very luminous in IR but seems to be rather devoid of cool gas ($M_{HI} < 10^8$ $M_\odot$ = detection limit) despite a very high star-formation rate (Bergvall et al., 2000). This suggests that either the starburst is about to run out of fuel or the gas is to a large extent in molecular and ionised form as suggested by calculation. The outer isocontours are distorted out to very faint isophotal levels ($\mu_R \approx 26$ mag/arcsec^2) on broad-band images (Fig. 2 – right). This is still visible but less extended in the Hα line demonstrating that the light originates mainly in stars. Hence, the large-scale distribution of stars in this galaxy is highly asymmetric. At all isophotal levels an extension in the south-east is evident. This may be a tidal tail in development or most likely the remnants of such.

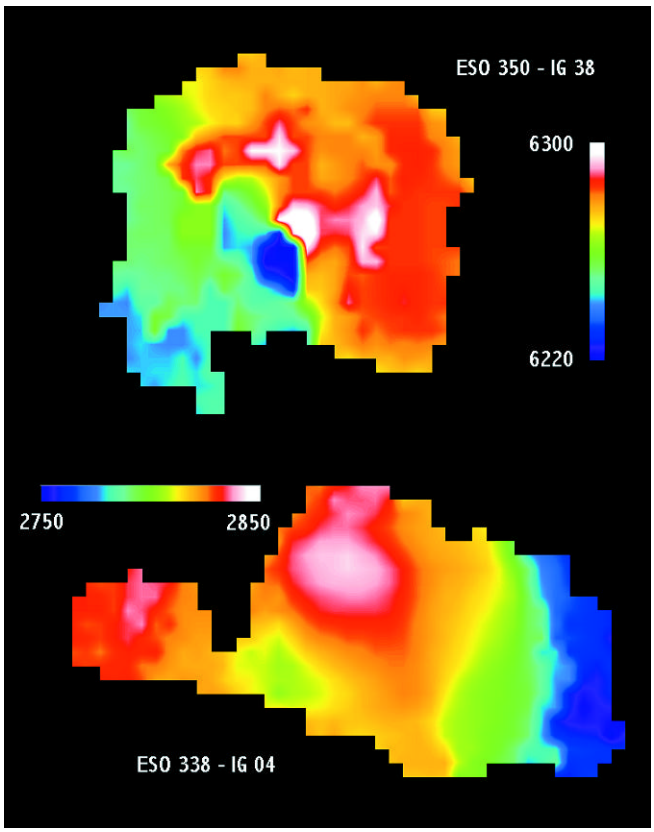

Figure 3: Velocity fields for ESO 350-IG38 (up) and ESO 338-IG04 (bottom). The two galaxies have the same pixel size (0.91 arcsec/px) and scale on the image; the horizontal size of the box is 42 arcsec. ESO 350-IG38: The velocity amplitude ranges linearly from violet (6220 km s^{-1}*) to white (6300 kms*$^{-1}$*). ESO338-IG04: The velocity amplitude ranges linearly from violet (2750 km s*$^{-1}$*) to white (2850 km s*$^{-1}$*).*

The Hα line profiles of this galaxy are broad, up to FWHM = 270 km/s, and have non-gaussian shape. This suggests that two or more non-virialised components may be present. In the centre, double peaked lines are present consistent with the presence of a counter rotating disk or high velocity blobs. This galaxy presents a strong central velocity gradient and large-scale distortions (see Fig. 4 – up). If we do not decompose the velocity field in several components, the rapid increase of the rotation curve is followed by a keplerian decrease. Alternatively, if we disentangle two possible components, the main one (in terms of intensity and extension) provides a low-velocity amplitude flat rotation curve while the second one gives a high-velocity amplitude but only in the central parts of the galaxy (see Fig. 5 – left). These properties indicate that the centre is not dynamically relaxed, while the outer velocity field shows a very slow rotation. The estimated stellar mass density exceeds by far what can be supported by the observed amount of rotation (G 30 km/s). Thus the galaxy is either not in equilibrium, or it is not primarily supported by rotation. These properties strongly suggest that the starburst has been triggered by a merger process.

3.2 ESO 338-IG04 (Tololo 1924-416)

HST observations of this well-known starburst (see Fig. 4 – left, Östlin et al., 1998) have revealed that in addition to

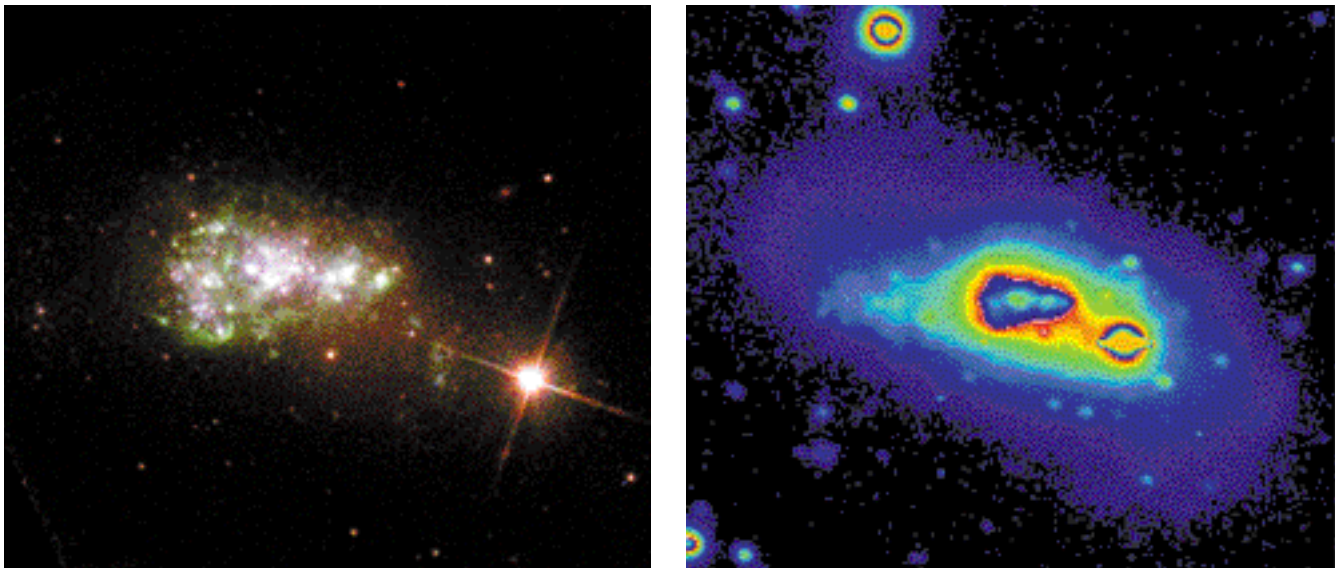

Figure 4: ***ESO 338-IGO4.*** *North is up, East is left. (Left): HST/WFPC2 true composite colour BVI-image. The scale of the box is 28 arcsec square. (Right): R-band CCD image. Note the irregular morphology at all isophotal levels. The faintest visible structures are* $\mu_R \approx$ *26 mag/arcsec*^{2}*. The size of the field is 60 arcsec* × *53 arcsec, corresponding to 11* × *9.5 kpc.*

many young compact star clusters, it contains a system of intermediate-age (~ 2 Gyr) globular clusters, a fossil of a previous dramatic starburst event. This galaxy has a companion at a projected distance of 70 kpc to the south-west. There is a 5 kpc long tail towards east, and large-scale isophotal asymmetries down to the μ_R = 26 mag/arcsec^2 level (Fig. 4 – right). At fainter levels, the morphology becomes more regular, but a boxy shape remains on the western side. The tail has much bluer colours than the rest of the galaxy outside the starburst region, signifying a younger stellar population. It contains stellar clusters, and cannot be explained by a purely gaseous tail.

This galaxy has an almost chaotic velocity field (see Fig. 3 – bottom), with strong gradients and an extended tail with little internal velocity structure. Approximately 10 arcsec east of the centre, just at the border of the central star-forming region, there is a velocity component whose kinematical axis is perpendicular to the photometric major axis of the galaxy (Figs. 5 and 6 in Östlin et al., 1999). The radial light distribution indicates that the observed mean rotational velocity (if a such is at all meaningful to define in view of the irregular velocity field) cannot support the system gravitationally. The tail has almost no velocity gradient with respect to the centre ($\Delta\upsilon \leq$ 10 km/s). On the other hand, the western half of the galaxy has a strong gradient and an implied rotational velocity of 80 km/s at a distance of 3 kpc from the centre. This is identical to the rotational velocity in the companion ESO 338-IG04B that has an equal photometric mass. Hence, the western part of the galaxy shows about the expected level of velocity difference with respect to the centre for rotational support to be possible. But what is happening at the eastern side in the tail? The colour of the tail suggests that it has a distinctly different stellar population from the rest of the galaxy. The most likely is that the tail is a remnant of a merger and that projection effects prevent us from seeing the true velocity amplitude. The part of the galaxy on the eastern side which is not in the tail, does not emit strongly in Hα, hence we have no information on its kinematics. Where the tail meets the starburst region, we see an increased Hα velocity dispersion, perhaps due to a shock. This coincides with the location of the perpendicular dynamical component discussed above. The companion is probably too far away for tidal forces to influence the internal gas kinematics to such an extent that it may have caused the starburst and the peculiar velocity field.

Radio interferometric observations (Östlin et al., in preparation) reveal that the galaxy is embedded in a very large HI cloud, more than 7 arcminutes across (corresponding to 80 kpc at the distance of ESO 338-IG04). The HI cloud has irregular morphology with two main components and no single axis of rotation. ESO 338-IG04 appears to be located in the eastern HI cloud. The companion is detected in HI but lies further away. Although we cannot exclude that the starburst in ESO 338-IG04 is triggered by interaction with the companion, a merger appears more likely in view of the complex velocity field and the non-rotating arm.

4. Discussion on the Whole Sample

4.1 Photometric and kinematical analysis

The morphologies of the BCGs present strong large-scale asymmetries down to the faintest isophotal levels, revealing large-scale asymmetries in the distribution of stars. In most cases we see clear signatures of merging/interaction. The young burst population dominates the integrated optical luminosities, while only contributing 1 to 5% of the total stellar mass, which ranges from a few times 10^8 to more than 10^{10} $M_\odot$. The mass is dominated by an older underlying population and the integrated (burst + old population) mass to light ratios are $M/L_V \sim 1$.

The velocity fields, in spite of the high signal-to-noise ratio of the emission lines, appear irregular and distorted, except for the two companion galaxies included in the sample. As the S/N is high, these irregular isovelocities should be considered as real. Some rotation curves appear strange or non-uniform; this indicates that the simple assumptions of a regular warp-free disk and pure circular motion around the centre are not valid in general. The estimated dynamical masses ranges from a few times 10^8 to a few times 10^9 $M_\odot$. Secondary components have been detected in several cases.

In about half the cases, the observed rotational velocities are too small to allow for pure rotational support. A possible explanation is that velocity dispersion dominates the gravitational support. This is consistent with the observed line widths ($\Delta_{H\alpha}$ = 35 to 80 km/s), but does not explain the strange shape of many of the rotation curves (see Fig. 5). Another possibility is that the galaxies are not in dynamical equilibrium, e.g. because they are involved in mergers, explaining the peculiar kinematics. It is also possible that gas and stars are dynamically decoupled and the Hα velocity field does not trace the gravitational potential. A way to distinguish between these alternatives would be to obtain the rotation curve and velocity dispersion for the

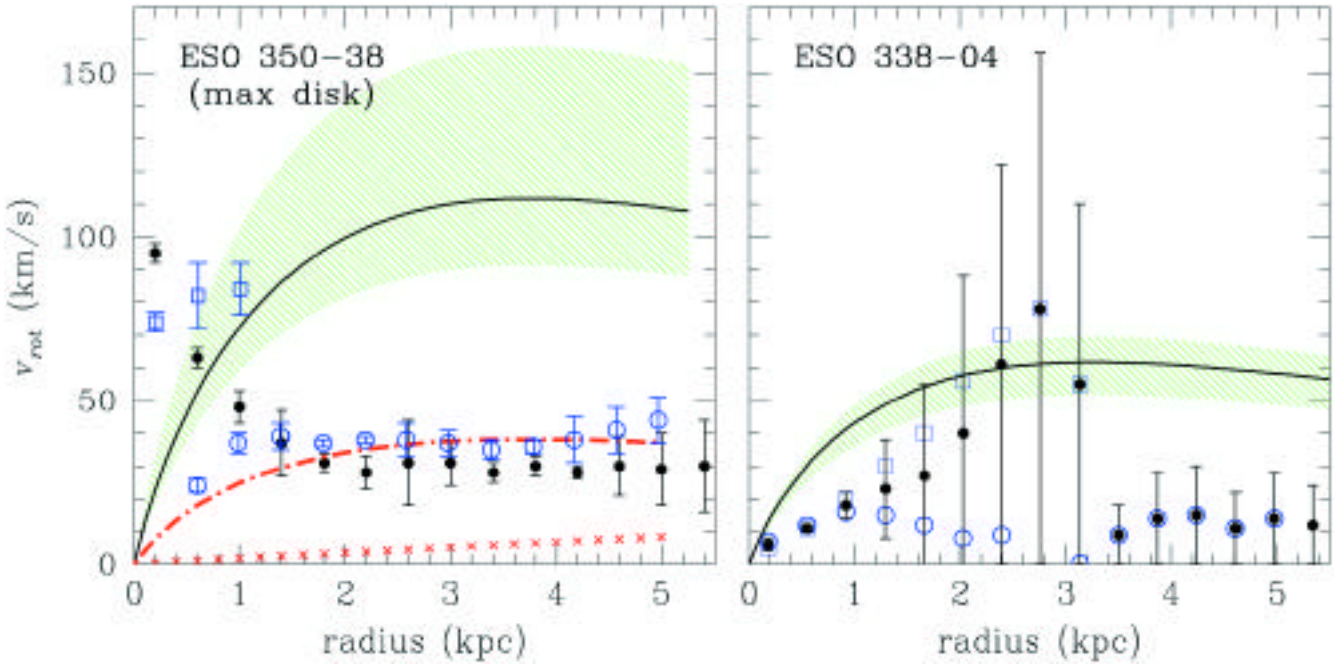

Figure 5: Mass model for ESO 350-IG38 (left) and ESO 338-IG04 (right). The solid line is the photometric rotation curve for the disk component; and the green shaded area is the allowed range based on the uncertainty in M/L. The filled circles show both sides'averaged observed rotation curves, the error bars represent mainly the deviation to pure circular motions. ESO 350-IG38 (left): the blue open symbols show the rotation curve based on the decomposed velocity field. The blue open circles correspond to the main component; the secondary component, which is counter rotating is shown by the blue open squares. The maximum disk model (in order to provide an upper limit of the (M/L)disk) has been computed on the main component. The dash-dot red line is the stellar disk component from the mass model and the crosses is the halo component (red crosses). As the halo component is very faint, the total model (disk + halo) matches the stellar component. ESO338-IG04 (right): The blue open symbols show both sides of the rotation curve. The blue open circles correspond to the receding side while the approaching one is shown by the blue open squares. Due to the disagreement between the approaching and the receding sides, the averaged rotation curves do not represent the axisymmetric potential well of the galaxy, the instrumental accuracy of the velocity being 2–3 km/s at high signal-to-noise ratio. Furthermore, no dynamical model can be plotted for this galaxy.

stellar component. In two cases, we find evidence for the presence of dark matter within the extent of the Hα rotation curves, and in two other cases we find marginal evidence. Indeed, even with a maximum disk model, the rotation curves computed from the surface brightness profiles cannot fit the observed rotation curve without an additional dark halo component.

4.2 Spectral Evolutionary Models and Dynamical Analysis

Spectral evolutionary synthesis models in combination with colour profiles in the optical and near infrared are used to estimate the mass to light ratios (M/L) of the galaxies (the models are described in Bergvall and Rönnback, 1995). Photometric mass distributions were derived by integrating the luminosity profiles for the disk and burst components and using their corresponding M/L values. The photometric mass distributions are further compared to dynamical mass models (see Fig. 5). From B-band surface brightness photometry, an exponential disk has been separated from the burst by extrapolation of the profile of the outer regions where the contribution to the burst is marginal. The photometric M/L of the disks and of the bursts have been evaluated by matching the observed colours to extended sets of models with different IMF, mass limit and star-formation histories (Östlin et al., 2001). The photometric total masses of the disk and of the burst have been obtained by integrating the luminosities with the M/L values in the allowed range. The dynamical M/L of the disk have been computed using a two-component (exponential disk + dark halo) best-fit mass model or maximum disk model (Carignan, 1985). In most cases, the M/L obtained from the dynamical mass models are lower than the ones obtained from the spectral evolutionary synthesis models. This means that the dynamical mass is under-evaluated, the velocity fields being disturbed by non-circular motions or/and that the galaxies are not rotationally supported.

4.3 Merging in Process

For this sample of LBCGs, two kinds of perturbation are probably in competition: (1) merging processes distorting the velocity fields at large scale and (2) winds driven by starbursts strongly disturbing the circular motion of the ionised gas at smaller scales. Merging, interaction and wind driven by supernovae can induce non-circular motions of high amplitude to the gas. Then, due to dissipative collisions, the gas is probably decoupled from the rotation of the stars which constitute the dominant mass of the disk. Stars and gas are then decoupled due to dissipative collisions in the gaseous component of the galaxies. Furthermore, the gas becomes a bad tracer of the potential well but a good tracer of starburst activity. Stars should be a better tracer of the potential well but their observations present difficulties due to the weakness of the continuum emission and absorption lines in this class of galaxies.

When considering the kinematics and morphologies of this sample of luminous BCGs, we are led to the conclusion that dwarf galaxy mergers are the favoured explanation for the starbursts. The dynamics of the studied galaxies fall into two broad classes: one with well behaving rotation curves at large radii and one with very perturbed dynamics. This may indicate a distinction of the fate of these galaxies, once the starbursts fade. Alternatively, depending on the state in which we see the interaction/merger, we will detect more or less chaotic velocity maps.

5. Perspectives

Dwarf galaxies are very common objects in the universe; compact galaxies (CGs) are frequent and blue compact galaxies (BCGs) are not rare. At high redshift, gas-rich dwarf galaxies and perhaps also CGs even can be the building blocks of the larger galaxies, merge and form stars during episodic processes in their evolution. The luminous blue compact galaxies (LBCGs)

ESO VACANCY

Applications are invited for the position of

Head of the Office for Science

Assignment: A strong research-oriented scientific staff with diverse expertise is essential to fulfil ESO's mandate of providing and maintaining international competitive observatories for its community of users. In this context the Head of the Office for Science will be responsible to the Director General for the science policies, and the main tasks will be

- to foster science across the entire Organisation and increase the exchange between ESO Chile and Garching;
- to support the efforts of ESO staff to conduct science at a high level;
- to provide a reference point for young scientists;
- to pursue actively the Fellowship, Studentship, Visitor programmes and carry out scientific exchanges with the European community through a strong and attractive Workshop Programme;
- to be the ESO representative at the International Research School recently created in the Munich area.

Experience and knowledge: Candidates must have an outstanding record of achievement in one or more areas of modern astrophysics and preferably be widely experienced in the use of large ground-based optical and/or radio telescopes. Excellent communication and management skills and a strong sense of team spirit are essential.

Duty station: Garching near Munich, Germany, with regular trips to Chile.

Starting date: 1 September 2001 or later.

We offer an attractive remuneration package including a competitive salary (tax free), comprehensive social benefits and financial help in relocating your family. The initial contract is for a period of three years with the possibility of a fixed-term extension. Serious consideration will be given to outstanding candidates willing to be seconded to ESO on extended leaves from their home institutions. Either the title or the grade may be subject to change according to education and the number of years of experience.
If you are interested in working in areas of front-line science and technology in a stimulating international research environment, please send us your CV (in English language) and the ESO Application Form (to be obtained from the ESO Home Page at http://www.eso.org/) and four letters of reference

before 15 May 2001.

For further information, please consult the ESO Home Page.

have luminosities and properties similar to galaxies seen at intermediate redshifts (e.g. Guzman et al., 1997). Moreover, they are among the least massive/luminous galaxies that are possible probes also at high redshifts. The sample of LBCGs presented here is not representative of classical BCGs but can be regarded as a reference sample for high redshift LBCGs, for which, moreover, observations present a serious bias. Even if there are evolutionary processes that make distant galaxies unique, the evolutionary history of a galaxy is not only a time-dependent parameter but it may also strongly depend on the environment. Furthermore, LBCGs can be thought of as nearby sites which mimic galaxy interaction, merging and the star triggering in higher-density environments of the young universe.

These local dwarf galaxy mergers may be the best analogues of hierarchical build-up of more massive galaxies at high redshifts.

Acknowledgements

We would like to thank our collaborators Nils Bergvall, Josefa Masegosa, Jacques Boulesteix and Isabel Marquez for their contributions to this work. Jean-Luc Gach from Marseille Observatory is thanked for providing the computations for Figure 1. Nils Bergvall is thanked for his comments and his careful reading of this paper. The 3.6-m ESO and the astroworkshop teams are thanked for providing efficient support during the set-up of the instrument.

References

Amram P., Boulesteix J., Georgelin Y.M. et al., 1991, *The Messenger*, **64**, 44.

Amram P., Balkowski C., Boulesteix J. et al., 1996, *A& A*, **310**, 737.

Bergvall N. and Olofsson K., 1984, *The Messenger* **38**, 2.

Bergvall N., Masegosa J., Östlin G. and Cernicharo J., 2000, *A&A* **359**, 41.

Bergvall N., Rönnback J., 1995, *MNRAS* **273**, 603.

Carignan C., 1985, *ApJ* **299**, 59.

Östlin G., in "Massive Stellar Clusters", A. Lancon and C. Boily Eds., 2000, ASP Conf. Ser. **211**, p. 63.

Östlin G., Amram P., Masegosa J., Bergvall N., Boulesteix J., 1999, *A&AS*, **137**, 419.

Östlin G., Amram P., Masegosa J., Bergvall N., Boulesteix J. and Marquez I. 2001, to be submitted.

Östlin G., Bergvall N., Rönnback J., 1998, *A&A* **335**, 85.

Gach J.L. et al., 2001, in preparation for *ApJS*.

Guzman R., Gallego J., Koo D.V. et al., 1997, *ApJ.* **489**, 559.

Georgelin Y.M., Russeil D., Amram P. et al., 2000, *A& A* **357**, 308.

Malkan, Gorjian and Tam, 1998, *ApJS* **117**, 25.

Marcelin, M.; Boulesteix, J.; Courtes, G.; Milliard, B. Nature, vol. 297, May 6, 1982, p. 38–42.

Searle L. and Sargent W.L.W., 1972, *ApJ.* **173**, 25.

Whitmore B., Schweizer F., 1995, *AJ* **109**, 960.